

The Higher Order Modal Characteristics of Circular–Rectangular Coaxial Waveguides

Haiyin Wang, Ke-Li Wu, *Senior Member, IEEE*, and John Litva, *Senior Member, IEEE*

Abstract—A rigorous analysis combining the orthogonal expansion method and Galerkin method for the higher order eigenmodes in a circular–rectangular (C-R) waveguide is presented in this paper. The Bessel–Fourier series is employed to merge the circular and rectangular coordinate systems used in the analysis. The cutoff frequencies of the higher order modes are determined with the singular value decomposition (SVD) technique. The computed results are in excellent agreement with results obtained using the finite element method. Because of its analytic form, the solution will be useful in the rigorous analysis of many practical microwave components and circuits.

I. INTRODUCTION

THE circular–rectangular (C-R) coaxial waveguide has been widely used in various microwave components and circuits due to its great compatibility with both circular coaxial waveguide and rectangular waveguides. However, there lacks a complete understanding of the electromagnetic characteristics involved. Many practical problems currently encountered could be better investigated if a complete knowledge of the eigenvalue spectrum of the C-R coaxial waveguide were known.

An example of a C-R coaxial waveguide transition is given by the input/output probe of coaxial waveguide combine filters or diplexer. Here, the TEM mode in a circular coaxial transmission line is coupled with the evanescent modes in a rectangular waveguide. Since all the higher order modes in a rectangular waveguide contribute to the coupling of evanescent modes, the effect of higher order modes in the C-R coaxial waveguide transition must be taken into account in a full electromagnetic analysis. In addition, information on higher order modes is also important for predicting the electromagnetic compatibility (EMC) characteristics of the C-R coaxial line-like structures (usually with multiple inner conductors) in high speed digital circuits. In particular, the latter is an interesting problem, where solutions will contribute to the development of today's high speed computers and switches in telecommunications.

The previous work is preceded by the work of Gruner [1], who used the Galerkin method to solve for the modes of a rectangular coaxial waveguide. The Galerkin method has also been successfully applied to the crossed rectangular waveguide

problem by Tham [2]. The solutions of these basic waveguide configurations have been widely used in characterizing various complicated microwave systems. For example, they have been applied to integrated antenna beamforming networks [3] and waveguide dual mode filters [4]. Nevertheless, since all these configurations can be described using a rectangular coordinate system, it is difficult to extend the solutions to the case of C-R coaxial waveguide, where one must introduce a cylindrical coordinate system. In 1991, Omar and Schünemann developed an approach to characterize the EM field in the C-R waveguide using summation of the eigenfunctions [5]. The eigenmode functions in the Cartesian coordinate system are transformed to the cylindrical coordinate system for integration along the inner circular conductor. To ensure the computational accuracy, many modes (probably 50 or more) have to be calculated in Omar's method. The previous work is based on a mono-coordinate system, either rectangular or cylindrical, and thereby improvement could be made by introducing a mixed C-R coordinate system for the C-R waveguide structure.

In this paper, a general mathematical expression of the higher order modes in a C-R coaxial waveguide is given in an explicit analytic form. The modal functions obtained are in the form of the Fourier series which can be conveniently used for further numerical manipulation. The Galerkin method is employed to formulate the problem. Because the formulation involves both rectangular and circular coordinate systems, the Bessel–Fourier series is used to merge the two different coordinate systems. In the proposed formulation, the scale Helmholtz equations are converted into a generalized matrix eigenvalue formulation. The singular value decomposition (SVD) technique is then used to determine the eigenvalue spectrum, and subsequently the Fourier coefficients of the mode functions.

II. BASIC FORMULA

The purpose of our investigation is to characterize the higher order modes in the waveguide shown in Fig. 1. In this geometry, the inner circular conductor is concentric with the outer rectangular conductor. In Fig. 1, notations "a" and "b" denote the half width and the half height of the rectangular enclosure, respectively, and r_0 gives the radius of the inner cylindrical conductor.

To analyze the C-R waveguide, the cross section is divided into two regions, the rectangular Region I and the cylindrical Region II. We use rectangular coordinates in Region I, and cylindrical coordinates in Region II. Both coordinate systems

Manuscript received June 18, 1996; revised November 21, 1996.

H. Wang and J. Litva are with Communications Research Laboratory, McMaster University, Hamilton, Ont., Canada L8S 4K1.

K.-L. Wu is with Corporate R&D Department, COM DEV Ltd., Cambridge, Ont., Canada N1R 7H5.

Publisher Item Identifier S 0018-9480(97)01719-5.

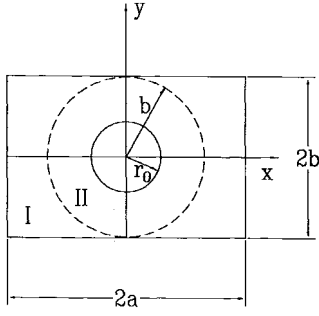


Fig. 1. Cross section of the C-R coaxial waveguide.

TABLE I
EIGENMODES DEFINITIONS

Mode	X axis	Y axis
TM _{odd, odd} , TE _{odd, odd}	Magnetic wall	Magnetic wall
TM _{odd, even} , TE _{odd, even}	Electric wall	Magnetic wall
TM _{even, odd} , TE _{even, odd}	Magnetic wall	Electric wall
TM _{even, even} , TE _{even, even}	Electric wall	Electric wall

have the same point of origin, which is located at the center of the inner conductor. The dashed line represents the imaginary boundary consisting of a cylindrical surface with radius b , which separates two regions.

The fields in Regions I and II are expressed in terms of eigenmode functions. We choose trigonometric functions and hyperbola functions in Region I, Bessel functions and trigonometric functions in Region II to represent the field distribution.

Since the structure of the waveguide is symmetrical with respect to the x and y axes, only one quadrant needs to be analyzed. Based on various boundary conditions which are assigned to the x and y axes for TM and TE modes, the eigenvalue problem can be divided into four distinct groups shown in Table I.

In Table I, the first/second subscript of the mode corresponds to the boundary conditions, which have been applied to the y/x axis, respectively.

In the later sections, the eigenvalue spectrum and the mode functions of each group are solved separately. By separating the modes into four groups, the mode spectrum becomes sparse. Therefore, the eigenvalues of the problem are much easier to locate.

A. Field Expression and Boundary Condition of TM Modes

In order to analyze the TM modes, the boundary conditions require the z component of the electric field intensity E_z to vanish along the outer and inner conductor surfaces. Therefore, E_z in Region I of the third quadrant can be expressed as

$$E_{zI} = \sum_{n=1,2,\dots}^{\infty} \psi_{In} \sinh \left[p_{In} \frac{x+a}{2a} \right] \sin \left[\frac{n\pi(y+b)}{2b} \right],$$

$$-a \leq x \leq 0, \quad -b \leq y \leq 0, \quad r > b \quad (1)$$

where

$$p_{In}^2 = -4k_c^2 a^2 + \left(\frac{n\pi a}{b} \right)^2 \quad (2)$$

here k_c is the cutoff wave number of the waveguide, which is written as

$$k_c^2 = \omega^2 \epsilon \mu - k_z^2 \quad (3)$$

and k_z is the propagation coefficient.

Because cylindrical coordinates are used in Region II, we express E_z in terms of the Bessel functions, i.e.,

$$E_{zII} = \sum_{m=0,1,\dots}^{\infty} \psi_{II m} [J_m(k_c \rho) Y_m(k_c r_0) - J_m(k_c r_0) Y_m(k_c \rho)] \Phi_m(\phi),$$

$$0 \leq \rho \leq b, \quad \pi \leq \phi \leq \frac{3\pi}{2} \quad (4)$$

The magnetic fields in Regions I and II can therefore be written as

$$H_{\phi I} = H_{yI} \cos \phi - H_{xI} \sin \phi$$

$$= -j \frac{\omega \epsilon}{k_c^2} \sum_{n=1,2,\dots}^{\infty} \psi_{In} \left\{ \frac{p_{In}}{2a} \cosh \left[p_{In} \frac{x+a}{2a} \right] \cdot \sin \left[\frac{n\pi(y+b)}{2b} \right] \cos \phi + \frac{n\pi}{2b} \sinh \left[p_{In} \frac{x+a}{2a} \right] \cdot \cos \left[n\pi \frac{y+b}{2b} \right] \sin \phi \right\} \quad (5)$$

$$H_{\phi II} = -j \frac{\omega \epsilon}{k_c^2} \sum_{m=0,1,\dots}^{\infty} \psi_{II m} |k_c| [J'_m(k_c \rho) Y_m(k_c r_0) - J_m(k_c r_0) Y'_m(k_c \rho)] \Phi_m(\phi) \quad (6)$$

where

$$\Phi_m(\phi) = \begin{cases} \cos(m\phi) \\ \sin(m\phi) \end{cases} \quad (7)$$

Obviously, the upper case of Φ_m corresponds to TM_{odd, odd} and TM_{even, odd} modes and the lower case corresponds to TM_{odd, even} and TM_{even, even} modes.

The continuity of E_z and H_{ϕ} implies that

$$E_{zI} = E_{zII}$$

$$H_{\phi I} = H_{\phi II} \quad (8)$$

at the imaginary boundary $\rho = b$.

After substituting the field expressions (1) and (4)–(6) into (8), we multiply both sides with eigen function $\Phi_k(\phi)$ in Region II and then integrate from π to $3\pi/2$. Because of the orthogonality between the trigonometric functions, the following equations are obtained

$$\sum_{n=1,3,\dots}^N \psi_{In} b_{ckn}^{tm} = \psi_{II k} e_k^{tm}$$

$$\sum_{n=1,3,\dots}^N \psi_{In} (e_{ckn}^{tm} + d_{ckn}^{tm}) = \psi_{II k} f_k^{tm} \quad (9)$$

where

$$b_{ckn}^{tm} = \int_{\pi}^{3\pi/2} \sinh \left[p_{In} \frac{b \cos \phi + a}{2a} \right] \cdot \sin \left[\frac{n\pi(\sin \phi + 1)}{2} \right] \cos(k\phi) d\phi \quad (10)$$

$$c_{ckn}^{tm} = \int_{\pi}^{3\pi/2} \frac{p_{In}}{2a} \cosh \left[p_{In} \frac{b \cos \phi + a}{2a} \right] \cdot \sin \left[\frac{n\pi(\sin \phi + 1)}{2} \right] \cos(\phi) \cos(k\phi) d\phi \quad (11)$$

$$d_{ckn}^{tm} = \int_{\pi}^{3\pi/2} \frac{n\pi}{2b} \sinh \left[p_{In} \frac{b \cos \phi + a}{2a} \right] \cdot \cos \left[\frac{n\pi(\sin \phi + 1)}{2} \right] \sin(\phi) \cos(k\phi) d\phi \quad (12)$$

$$e_k^{tm} = [J_k(kcb)Y_k(kcr_0) - J_k(kcr_0)Y_k(kcb)]\Delta_k \quad (13)$$

$$f_k^{tm} = |k_c| [J'_k(kcb)Y_k(kcr_0) - J_k(kcr_0)Y'_k(kcb)]\Delta_k \quad (14)$$

$$\Delta_k = \begin{cases} \frac{\pi}{2} & k = 0 \\ \frac{\pi}{4} & k \neq 0 \end{cases} \quad (15)$$

when $\Phi_k(\phi) = \cos(k\phi)$, and

$$\Delta_k = \frac{\pi}{4} \quad (16)$$

when $\Phi_k(\phi) = \sin(k\phi)$. In these equations, $n = 1, \dots, N$, $m = 1, \dots, M$, N , and M are the numbers of modes used in the Regions I and II.

After eliminating ψ_{In} from (9), the above equations results in

$$\mathbf{A}\psi_{II} = \mathbf{0} \quad (17)$$

where

$$\mathbf{A} = \mathbf{E}^{tm} - \mathbf{B}_c^{tm}(\mathbf{C}_c^{tm} + \mathbf{D}_c^{tm})^{-1}\mathbf{F}^{tm}. \quad (18)$$

The superscript -1 means the inverse of the matrix. The elements of each matrix are given by (11)–(16). To insure the existence of the inverse of the matrix, the numbers of modes used in Regions I and II should be the same, that is $M = N$.

To search for the nontrivial solution of (17), the determinant of matrix \mathbf{A} has to be equal to zero. A group of eigenvalues that satisfy the characteristic equation $\det[\mathbf{A}] = 0$ can be obtained. Each eigenvalue corresponds to a cutoff wavenumber for a higher order TM mode in the C-R waveguide. Consequently, the eigenmodes can be obtained from the solution for ϕ_{II} and ϕ_{In} .

The boundary conditions for TM modes on the x and y axes include: the tangential components of a magnetic field should be zero on the magnetic wall and the tangential components of a electric field should be zero on the electric wall. It means that $\partial E_z / \partial n$ needs to be zero along the x and y axes for $\text{TE}_{\text{odd, odd}}$ modes. We chose $\Phi_k(\phi) = \cos(k\phi)$ with $m = 0, 2, 4, \dots$ and $n = 1, 3, 5, \dots$. These satisfy the boundary conditions of the perfect magnetic wall along the x and y axes. For $\text{TE}_{\text{even, odd}}$ modes, we use the same $\Phi_k(\phi)$ with $m = 1, 3, 5, \dots$, $n = 1, 3, 5, \dots$.

Similarly, we can obtain the matrix equation for $\text{TM}_{\text{odd, even}}$ and $\text{TM}_{\text{even, even}}$ modes with $\Phi_k(\phi) = \sin(\phi)$, where $m = 1, 3, 5, \dots$, $n = 2, 4, 6, \dots$ for $\text{TM}_{\text{odd, even}}$ modes, and $m = 2, 4, 6, \dots$ and $n = 2, 4, 6, \dots$ for $\text{TM}_{\text{even, even}}$ modes.

The other components of electric fields, E_x , E_y , E_ρ , E_ϕ , and magnetic field components can be derived from E_z by using Maxwell's equations.

B. Field Expression and Cutoff Frequencies of TE Modes

For TE modes, $H_z \neq 0$ and $E_z = 0$. The magnetic field H_z for TE modes is given by

$$\mathbf{H}_{zI} = \sum_{n=0,1,\dots}^{\infty} \psi_{In} \cosh \left[p_{In} \frac{x+a}{2a} \right] \cos \left[\frac{n\pi(y+b)}{2b} \right], \quad -a \leq x \leq 0, \quad -b \leq y \leq 0, \quad (19)$$

$$\mathbf{H}_{zII} = \sum_{m=0,1,\dots}^{\infty} \psi_{II} [J_m(k_c \rho) Y'_m(k_c r_0) - J'_m(k_c r_0) Y_m(k_c \rho)] \Phi_m(\phi), \quad 0 \leq \rho \leq b, \quad \pi \leq \phi \leq 3\pi/2 \quad (20)$$

where

$$\Phi_m(\phi) = \begin{cases} \sin(m\phi) \\ \cos(m\phi) \end{cases}. \quad (21)$$

The upper case is for $\text{TE}_{\text{odd, odd}}$ and $\text{TE}_{\text{even, odd}}$ modes. The lower case is for $\text{TE}_{\text{odd, even}}$ and $\text{TE}_{\text{even, even}}$ modes.

Using $\Phi_k(\phi)$ for the inner product with $H_{zI} = H_{zII}$ and $E_{\phi I} = E_{\phi II}$, and eliminating ψ_{In} from the equations, we have the matrix (17) again with

$$\mathbf{A} = \mathbf{E}^{te} - \mathbf{B}_s^{te}(\mathbf{C}_s^{te} - \mathbf{D}_s^{te})^{-1}\mathbf{F}^{te} \quad (22)$$

where

$$b_{smn}^{te} = \int_{\pi}^{3\pi/2} \cosh \left[p_{In} \frac{b \cos \phi + a}{2a} \right] \cdot \cos \left[\frac{n\pi(\sin \phi + 1)}{2} \right] \Phi_m(\phi) d\phi \quad (23)$$

$$c_{smn}^{te} = \int_{\pi}^{3\pi/2} \frac{p_{In}}{2a} \sinh \left[p_{In} \frac{b \cos \phi + a}{2a} \right] \cdot \cos \left[\frac{n\pi(\sin \phi + 1)}{2} \right] \cos(\phi) \Phi_m(\phi) d\phi \quad (24)$$

$$d_{smn}^{te} = \int_{\pi}^{3\pi/2} \frac{n\pi}{2b} \cosh \left[p_{In} \frac{b \cos \phi + a}{2a} \right] \cdot \sin \left[\frac{n\pi(\sin \phi + 1)}{2} \right] \sin(\phi) \Phi_m(\phi) d\phi \quad (25)$$

$$e_{mm}^{te} = [J_m(kcb)Y'_m(kcr_0) - J'_m(kcr_0)Y_m(kcb)]\Delta_k \quad (26)$$

and

$$f_{mm}^{te} = |k_c| [J'_m(kcb)Y'_m(kcr_0) - J'_m(kcr_0)Y'_m(kcb)]\Delta_k. \quad (27)$$

We use $\Phi_k(\phi) = \sin(k\phi)$ for $\text{TE}_{\text{odd, odd}}$ modes and $\text{TE}_{\text{even, odd}}$ modes. In addition, $m = 2, 4, 6, \dots$, $n = 1, 3, 5, \dots$ for $\text{TE}_{\text{odd, odd}}$ modes, and $m = 1, 3, 5, \dots$, $n = 1, 3, 5, \dots$ for $\text{TE}_{\text{even, odd}}$ modes.

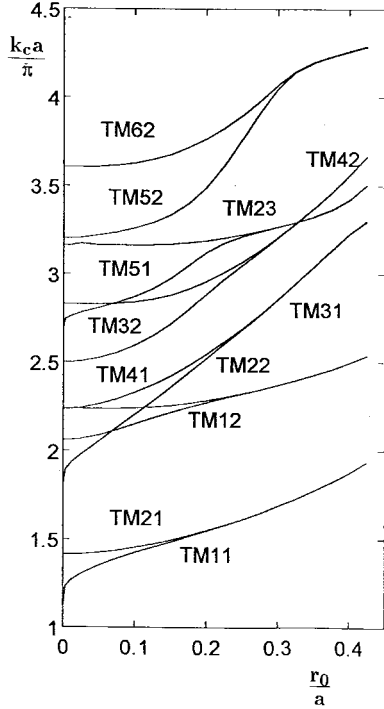


Fig. 2. Typical TM mode characteristics of C-R coaxial waveguide ($b/a = 0.5$).

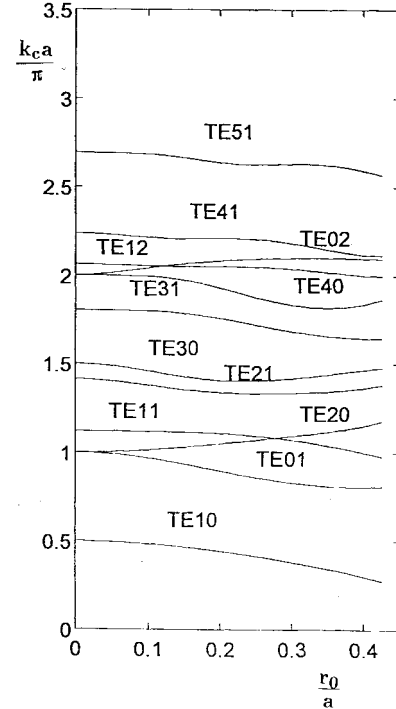


Fig. 3. Typical TE mode characteristics of C-R coaxial waveguide ($b/a = 0.5$).

Similarly, $\Phi_k(\phi) = \cos(k\phi)$ is used for $TE_{\text{odd, even}}$ modes and $TE_{\text{even, even}}$ modes, with $m = 1, 3, 5, \dots$, $n = 0, 2, 4, \dots$ for $TE_{\text{odd, even}}$ modes, and $m = 2, 4, 6, \dots$, $n = 0, 2, 4, \dots$ for $TE_{\text{even, even}}$ modes.

The values of Δ_k are also given by (15) and (16).

C. Bessel-Fourier Series

Using $sh(x) = (e^x - e^{-x})/2$, (10) can be rewritten as

$$b_{ckn}^{tm} = \int_{\pi}^{3\pi/2} \left\{ \frac{1}{2} e^{pIm} (b \cos \phi + a/2a) \sin \left[\frac{n\pi(\sin \phi + 1)}{2} \right] \cdot \cos(k\phi) - \frac{1}{2} e^{-pIm} [(b \cos \phi + a)/2a] \cdot \sin \left[\frac{n\pi(\sin \phi + 1)}{2} \right] \cos(k\phi) \right\} d\phi \quad (28)$$

We use the Bessel-Fourier series to calculate the above integrals analytically. The Bessel-Fourier series is given by [6]

$$\begin{aligned} & \sin \frac{n\pi(b + \rho \sin \phi)}{2b} e^{\mp \gamma_{xi} \rho \cos \phi} \\ &= \sum_{-\infty}^{\infty} \sin \left(\frac{n\pi}{2} + k\phi \right) \\ & \begin{cases} J_k[T(\rho)] \exp[\mp jk \arctan(2b|\gamma_{xi}|/m/\pi)], & \gamma_{mi}^2 < 0 \\ J_k[T(\rho)] \left[\frac{n\pi + 2b\gamma_{xi}}{n\pi - 2b\gamma_{xi}} \right]^{\mp k/2}, & m\pi > 2b|\gamma|, \gamma_{mi}^2 > 0 \\ (-1)^{k/2} I_k[|T(\rho)|] \left[\frac{n\pi + 2b\gamma_{xi}}{n\pi - 2b\gamma_{xi}} \right]^{\mp k/2}, & m\pi < 2b|\gamma|, \gamma_{mi}^2 > 0 \end{cases} \end{aligned} \quad (29)$$

$$\begin{aligned} & \cos \frac{n\pi(b + \rho \sin \phi)}{2b} e^{\mp \gamma_{xi} \rho \cos \phi} \\ &= \sum_{-\infty}^{\infty} \cos \left(\frac{n\pi}{2} + k\phi \right) \\ & \begin{cases} J_k[T(\rho)] \exp[\mp jk \arctan(2b|\gamma_{xi}|/m/\pi)], & \gamma_{mi}^2 < 0 \\ J_k[T(\rho)] \left[\frac{n\pi + 2b\gamma_{xi}}{n\pi - 2b\gamma_{xi}} \right]^{\mp k/2}, & m\pi > 2b|\gamma|, \gamma_{mi}^2 > 0 \\ (-1)^{k/2} I_k[|T(\rho)|] \left[\frac{n\pi + 2b\gamma_{xi}}{n\pi - 2b\gamma_{xi}} \right]^{\mp k/2}, & m\pi < 2b|\gamma|, \gamma_{mi}^2 > 0 \end{cases} \end{aligned} \quad (30)$$

where

$$\gamma_{xn}^2 = \left(\frac{n\pi}{2b} \right)^2 - k_c^2 \quad (31)$$

$$\begin{aligned} T(\rho) &= \frac{\rho}{2b} [(n\pi)^2 - (2b\gamma_{xn})^2]^{1/2} \\ &= \rho k_c. \end{aligned} \quad (32)$$

By using the Bessel-Fourier series, numerical integrations are eliminated from the inner products at the imaginary boundary. To ensure the accuracy of the summation, the number of the terms that are used must be at least as large as

$$K = 15 + 3n \quad (33)$$

III. NUMERICAL RESULTS AND DISCUSSION

In order to verify the modeling approach and demonstrate its application, a C-R waveguide is investigated in detail. The waveguide has dimensions of $a = 2.54$ cm and $b = 1.27$ cm. The cutoff frequencies are obtained by mapping the complete

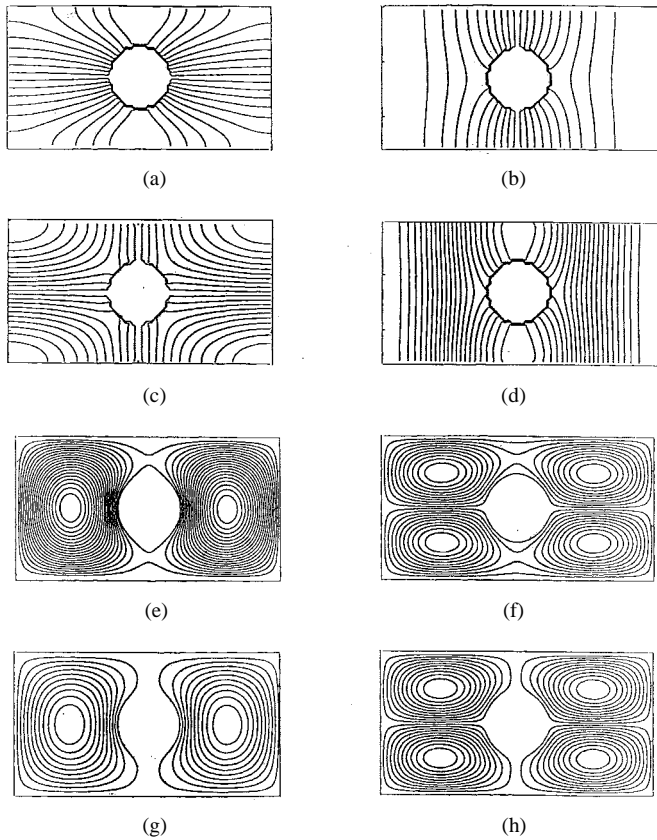


Fig. 4. Field configuration of TE and TM modes in a C-R coaxial waveguide: (a) TE₀₁ mode, (b) TE₁₀ mode, (c) TE₁₁ mode, (d) TE₂₀ mode, (e) TM₁₁ mode, (f) TM₁₂ mode, (g) TM₂₁ mode, and (h) TM₂₂ mode.

frequency range of interest for each mode. The SVD technique is used to determine the image points that satisfy the equation $\det(\mathbf{A}) = 0$ [7]. The advantage of the SVD technique is that it is able to improve the efficiency and reliability in the zero point searching procedure.

Figs. 2 and 3 show the cutoff wavenumbers k_c versus the normalized inner conductor radius r_0/a . It can be seen that the k_c of each TE or TM mode in the C-R waveguide approaches the value of a hollow waveguide of the same dimensions as r_0 approaches a value of zero. Therefore, the hollow rectangular waveguide may be viewed as a special case in the C-R waveguide modeling. There are a number of degenerate modes that share the same cutoff frequencies for $r_0 = 0$. The degenerate modes split as the inner conductor radius is increased (TE₀₁, TE₂₀, and TE₀₂, TE₄₀ in Fig. 2, TM₄₁, TM₂₂ in Fig. 3).

Another interesting phenomenon of the C-R waveguide is that when the inner conductor dimension r_0 increases, pairs of cutoff wavenumbers related to different TM modes converge (Fig. 3). This phenomenon implies a possibility that two TM modes can be combined or a single mode can be split in two by adjusting the r_0/a ratio. A possible explanation for this is that the two TM modes sharing the same second subscript are under the same x -axis boundary conditions but different y -axis conditions. Furthermore, one of the modes takes the y -axis as the electric wall while the other takes the y -axis as the magnetic wall. As r_0 increases, the boundary along the

TABLE II
COMPARATIVE ANALYSIS WITH RELATIVE DIFFERENCES FOR k_c VALUES

Modes	k_c (1/cm) by present method	k_c (1/cm) by finite element method	relative method
TE ₁₀	0.51124951	0.51147162	$4.34 * 10^{-4}$
TE ₀₁	1.0637058	1.06394546	$2.25 * 10^{-4}$
TE ₂₀	1.3253987	1.32524321	$1.17 * 10^{-4}$
TE ₁₁	1.3535700	1.35370480	$9.95 * 10^{-5}$
TE ₂₁	1.6493145	1.6493224	$4.78 * 10^{-6}$
TE ₃₀	1.7379933	1.7379533	$2.30 * 10^{-5}$
TE ₃₁	2.1282537	2.1285580	$1.42 * 10^{-4}$
TE ₄₀	2.3222497	2.3226796	$1.85 * 10^{-4}$
TE ₁₂	2.5335094	2.5335731	$2.51 * 10^{-5}$
TE ₀₂	2.5892876	2.5892433	$1.71 * 10^{-5}$
TM ₁₁	1.9948099	1.9935818	$6.16 * 10^{-4}$
TM ₂₁	1.9953650	1.9946881	$3.39 * 10^{-4}$
TM ₁₂	2.8694867	2.8691664	$1.11 * 10^{-4}$
TM ₂₂	2.8721777	2.8718947	$9.85 * 10^{-4}$
TM ₃₁	3.3197216	3.3178141	$5.74 * 10^{-4}$
TM ₄₁	3.3264943	3.3247878	$5.13 * 10^{-4}$
TM ₃₂	3.7715987	3.7705847	$2.68 * 10^{-4}$
TM ₄₂	3.7941012	3.7933216	$2.05 * 10^{-4}$
TM ₅₁	3.9728472	3.9723368	$1.28 * 10^{-4}$
TM ₂₃	3.9843494	3.9838875	$1.15 * 10^{-4}$

y -axis becomes shorter and shorter until eventually, the two modes become one.

In Fig. 4, is plotted the contours of the eight typical TM and TE modes in the waveguide, where $r_0/a = 0.225$. It is noted that the field distribution of each mode seems to be a modification of the corresponding mode field in a hollow waveguide.

In order to further verify the validity of this analytical method, we compared the k_c results with the values calculated with a finite element numerical technique. The waveguide size is $a = 2.54$ cm, $b = 1.27$ cm, and $r_0 = 0.635$ cm. The average element size in the finite element method is 0.1016 cm. Table II gives the comparison for each mode in the waveguide, and the relative error between the two method is less than $9.85 * 10^{-4}$.

IV. CONCLUSION

A general analysis has been presented for a C-R coaxial waveguide. The mathematical expressions for the higher order modes in the waveguide are derived using the Galerkin method based on two different coordinate systems. It is easy to determine the eigenvalue spectrum of the higher order modes using the formula given in the paper. The cutoff frequencies and the eigenmodes in the waveguide are solved through SVD. The numerical results agree with the results of finite element method.

The method can be extended to the case of an off-centered circular conductor by using the addition theorems of Bessel functions. The further extension is under developing.

ACKNOWLEDGMENT

The authors would like to thank Dr. X.-P. Liang of Allen Telecom Group for his valuable discussions.

REFERENCES

- [1] L. Gruner, "Higher order modes in rectangular coaxial waveguides," *IEEE Trans. Microwave Theory Tech.*, vol. MTT-15, pp. 483-485, Aug. 1967.
- [2] Q. C. Tham, "Modes and cutoff frequencies of crossed rectangular waveguides," *IEEE Trans. Microwave Theory Tech.*, vol. MTT-25, pp. 585-588, July 1977.
- [3] F. Alessandri, M. Mongiardo, and R. Sorrentino, "Computer-aided design of beam forming networks for modern satellite antennas," *IEEE Trans. Microwave Theory Tech.*, vol. 40, pp. 1117-1127, June 1992.
- [4] K.-L. Wu and R. H. Macphie, "A rigorous analysis of a cross waveguide to large circular waveguide junction and its application in waveguide filter design," *IEEE Trans. Microwave Theory Tech.*, to be published.
- [5] A. S. Omar and K. F. Schünemann, "Application of the generalized spectral-domain technique to the analysis of rectangular waveguides with rectangular and circular metal inserts," *IEEE Trans. Microwave Theory Tech.*, vol. 39, pp. 944-952, June 1991.
- [6] X. P. Liang, "Modeling of dual mode dielectric resonator filters and multiplexers," Ph.D. dissertation, Univ. Maryland, 1993.
- [7] V. A. Labay and J. Bornemann, "Singular value decomposition improves accuracy and reliability of T-septum waveguide field-matching analysis," *Int. J. Microwave Millimeter-Wave Computer-Aided Eng.*, vol. 2, no. 2, pp. 82-88, 1992.



Haiyin Wang received the degree in electrical engineering from the University of Science and Technology of China, Hefei, China. She received the M.E.E.E degrees from Tsinghua University, China, and Memorial University, Canada, respectively. She is now working toward the Ph.D. degree at McMaster University, Hamilton, Ont., Canada.

From 1983 to 1988, she worked as an electrical engineer at the Chinese Academy of Space Technology, Beijing, China, doing research on signal propagation between the ground station and the satellite and designing antennas for satellites and radars. Her current research interests include modeling and design of microwave devices and circuits.



Ke-Li Wu (M'90-SM'96) received the B.S. and M.S.E. degrees from the East China Institute of Technology, China, in 1982 and 1985, respectively, and the Ph.D. degree from Laval University, Canada, in 1989, all in electrical engineering.

From 1989 to 1990, he was a Post-Doctoral Fellow at McMaster University, Hamilton, Ont., Canada. He joined the Integrated Antenna Group, Communications Research Laboratory, McMaster University, in 1990 as a Research Engineer. Since 1991, he has been an Assistant Professor of Electrical and Computer Engineering at McMaster University. He joined COM DEV Ltd., Cambridge, Canada, in March 1993, where he is a Senior Member of the Technical Staff in the Corporate R&D Department. His present fields of interest include all aspects of numerical methods in electromagnetics with emphasis on rigorous analysis of waveguide systems, integrated antennas, and microwave integrated circuits. He contributed to *Finite Element and Finite Different Methods in Electromagnetic Scattering*, Volume 2 of *Progress in Electromagnetics Research* (Elsevier, 1990) and to *Computational Electromagnetics* (North-Holland, 1991). He has also published more than 20 journal papers.

Dr. Wu received a URSI Young Scientist Award in 1992.



John Litva (SM'92) is currently a Professor in Electrical and Computer Engineering at McMaster University, Hamilton, Ont., Canada. He is a Thrust Leader for the Telecommunications Institute of Ontario (TRIO), a university-industry based Center of Excellence funded by the Province of Ontario, to conduct research in support of Ontario's telecommunications industry. He is also the Director of the Communications Research Laboratory (CRL) at McMaster University. CRL carries out research in signal processing, software engineering, network-

ing, microwaves, computer modeling, and antennas. His present research interests are in LMDS, smart antennas for wireless, electromagnetic modeling, and propagation measurements and modeling.